

# Theoretical analysis of a methane gas detection system, using using the complementary source modulation method of correlation spectroscopy

Paul Chambers, Ed A. D. Austin and John P. Dakin

Optoelectronics Research Centre, University of Southampton, Southampton, UK

**Abstract.** Results from simulations of the response of a methane gas sensor using optical correlation spectroscopy (CoSp) are presented. Predictions of the sensor response, signal/noise performance and detection sensitivity are made for a typical fibre optic-coupled system. Spectral absorption data of the gases is obtained from the publicly available HITRAN database. Emphasis is placed on the effects on the detection sensitivity of varying (a) the optical filter characteristics, i.e. center wavelength and bandwidth, and (b) the concentration (partial pressure) of CH<sub>4</sub> gas. Using a 150 nm filter, and assuming a received optical power density at the detector of 10 nW nm<sup>-1</sup>, a theoretical noise-limited detection limit below 1 ppm is predicted. The cross-sensitivity to water vapor is derived and compared to that which would occur with a conventional broadband absorption method, i.e. one that would not exhibit the same selectivity as the CoSp method. This work is important for predicting the responsivity, sensitivity and crosstalk performance of practical CoSp gas detection systems.

## 1. Introduction

Optical absorption based Correlation Spectroscopy (CoSp) is a means of selectively detecting, or "fingerprinting", gases of industrial importance, which has the advantage of being inherently self-referencing to the various factors that might cause optical intensity changes (eg. light source variations, bending loss in fibers, etc.). A complete theoretical model of such a system for the measurement of methane (CH<sub>4</sub>) gas is presented. This is used to predict the fractional changes (modulation index) in the detected response which are expected when gases are introduced into the sensor. The predicted system Signal-to-Noise Ratio (SNR) and the expected Noise-Limited Detection Sensitivity (NLDS) is calculated, taking into account the effects of the fundamental photon noise limitations and practical thermal noise contributions. The cross-sensitivity performance due to water vapor contamination is also derived. Gas transmission spectra for these calculations were obtained from the publicly available HITRAN database (<http://www.hitran.com>).

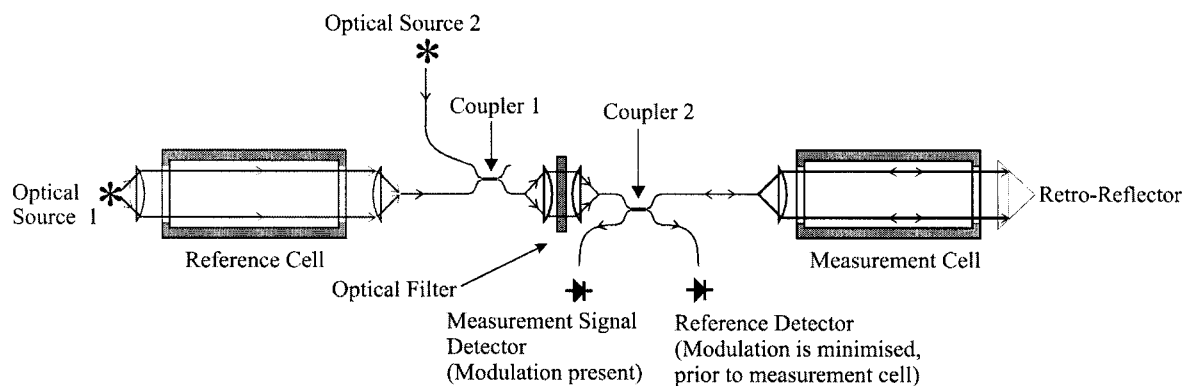


**Figure 1.** Schematic of a fibre optic based implementation of an absorption based correlation spectroscopy system.

## 2. Principle of operation

There is a wide variety of methods for detecting gases using correlation spectroscopy [1, 2, 3, 4, 5, 6, 7, 8, 9]. An attractive absorption-based option is the Complementary Source Modulation (CoSM) variant of the generic CoSp method [10, 11, 12]. This involves the alternate on/off switching of two light sources in anti-phase, passing the light from one of these sources through a reference cell containing the target gas (or gases) of interest, and then combining this now partially-absorbed light beam with a fraction of unaffected light from the other source, in a proportion such as to give no net intensity modulation. This equalization of beam power is performed after both beams have been appropriately filtered to match the absorption band of the target gas. The combined and filtered beam is then used to probe for the target gas.

As the beam component which has passed through the reference gas sample now has less available optical energy lying within the narrow spectral region of the target gas absorption lines, a net intensity modulation of the balanced combined beam will be re-established when it passes through a measurement cell, provided this contains the gas of interest. This induced intensity modulation is proportional to the target gas absorption level, as only differential absorption between the two beam components can contribute to the signal modulation. A fibre optic based schematic of an absorption based CoSp gas sensing system is shown in figure 1. The input signal detector is used to ensure balanced light power in the combined beam, and the output signal detector is used to evaluate any intensity modulation resulting from test gas in the measurement cell.

As might be expected, the characteristics of the filter used are important input parameters to any theoretical analysis of the system.

### 3. System model

It is important to model such a CoSp system, firstly to predict its performance, and secondly to choose the optical filter characteristics (or the spectral output desired from an LED or super-luminescent optical fibre source) that will result in the best detection performance or best selectivity. To do this, the parameters that determine the system performance must be defined.

We shall define the "modulation index", a normalized unit-less parameter, as the peak-to-peak AC signal variation that will arise at the output detector, when gas is introduced into the measurement cell, divided by the mean DC detector output level (the latter after subtraction of any DC offset signal that may be present under dark conditions). The modulation index is related to the transmission spectra of the reference cell,  $T_{Ref}(\lambda)$ , the measurement cell  $T_{Meas}(\lambda)$ , and the optical filter,  $F(\lambda)$ , as shown by equation 1.

$$m = 2 \left( \frac{\int F(\lambda)T_{Ref}(\lambda)T_{Meas}(\lambda)d\lambda \int F(\lambda)d\lambda - \int F(\lambda)T_{Ref}(\lambda)d\lambda \int F(\lambda)T_{Meas}(\lambda)d\lambda}{\int F(\lambda)T_{Ref}(\lambda)T_{Meas}(\lambda)d\lambda \int F(\lambda)d\lambda + \int F(\lambda)T_{Ref}(\lambda)d\lambda \int F(\lambda)T_{Meas}(\lambda)d\lambda} \right) \quad (1)$$

The source spectra has been assumed to be "flat", or wavelength independent, in equation 1, but it can also be taken into account by including further spectral functions as additional product terms. It is the integration of products of spectral transmission terms over a wavelength interval that justifies the use of the term **correlation** spectroscopy to describe the method.

The modulation index present when the measurement cell is filled with target gas is a measure of the optical 'contrast'. It is practically desirable to have a high modulation index to reduce the sensitivity of detected power to environmental effects, such as dust in sensing cells or mechanical vibration. However, it is not the only practical factor, as a high Signal-to-Noise Ratio (SNR) is fundamentally necessary to achieve high gas detection sensitivity.

The SNR is defined as the ratio of the optical signal change resulting when gas is introduced into the cell, to the random noise level in this signal, after bandwidth reduction due to time-averaging of the signal over the desired system response time. For practical reasons, the maximum convenient period for the latter is typically of order of 10 seconds. If there are no environmental or intensity changes in the optical signal, then it is only this SNR factor and the nature of the gas absorptions in each cell that together determine the fundamental limit to the minimum gas detection level.

The effects of the modulation index, signal to noise ratio and resulting gas detection sensitivity that occur when changing the optical filter ( $F(\lambda)$ ) characteristics, i.e center wavelength and full width at half maximum (FWHM) bandwidth will be analyzed below, making assumptions regarding the received optical power levels at the detector.

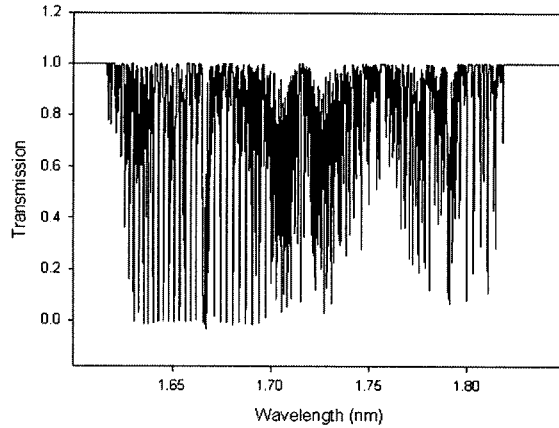


**Figure 2.** Transmission spectrum of CH<sub>4</sub> gas over a 1 m path length at STP (transmission data was obtained from the HITRAN database).

## 4. Numerical Results

In this section, the transmission spectrum of CH<sub>4</sub> gas is shown first, then results from the model will be used to predict the expected modulation index, the SNR in measurements, the measurement sensitivity and the cross-sensitivity to a contaminant gas (water vapor).

### 4.1. Transmission of CH<sub>4</sub> gas

Methane gas (CH<sub>4</sub>) exhibits a strong rotational-vibrational  $2\nu_3$  based absorption band at approximately  $1.7\mu\text{m}$ , the spectrum of which is shown in figure 2. Many commercially available optical sources and passive optical components function well in this wavelength range so it is relatively straightforward to implement optical systems for this spectral region.

### 4.2. Received modulation index (optical 'contrast')

It is intuitively expected that the highest modulation index should be achieved using a very narrow bandwidth line filter, centered on the strongest section of the CH<sub>4</sub> absorption spectrum. However, this would fail to make use of a significant proportion of the spectral power available from a broadband optical source, and would remove the inherent advantage of CoSp, that of "fingerprinting" the gas, i.e. operating using many absorption lines. In addition, such narrow-band operation on a single line can lead to severe problems with "speckle noise" - a type of amplitude noise due to multi-mode or multi-path interference. Bending of multimode fibers can cause very significant intensity changes due to modal noise effects when narrowband measurements are made, particularly bearing in mind the small fractional intensity changes that occur when

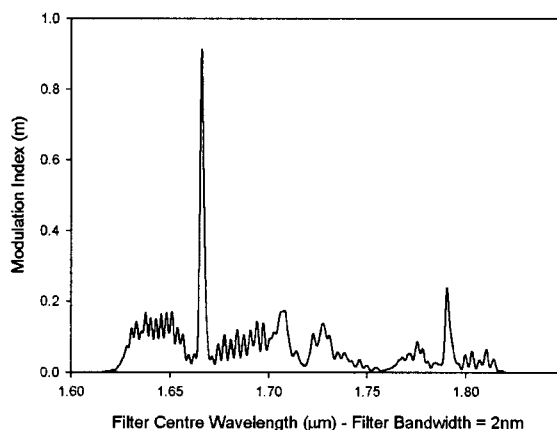


**Figure 3.** Modulation index as a function of selection filter center wavelength, assuming reference and measurement cells contain 100% CH<sub>4</sub> at 1.013 Bar and 20 °C and the Gaussian-shaped selection filter has a 2 nm FWHM bandwidth.

measuring low levels of gas. Unfortunately it is very difficult to model such noise and the level of which will only become apparent in an engineered system. However, a reduction in the coherence of light is generally a good way of avoiding this troublesome problem.

It is clear, therefore, that the choice of optical filter center wavelength and bandwidth, and its effect on the modulation index, SNR, selectivity and source coherence must be considered with great care.

Initially, to investigate the choice of center wavelength, we shall take a filter with a Gaussian shaped transmission function and FWHM (Full Width at Half Maximum) bandwidth of 2 nm, and scan the center wavelength over the full region of the CH<sub>4</sub> band. This filter is broad enough to include the effect of more than one absorption line, yet is sufficiently narrow to still show the main shape of the envelope of the absorption band. The resulting graph gives a better visual indication of the regions of higher average absorption than can be easily seen from a high resolution spectrum. Figure 3 plots the modulation index as a function of wavelength, giving a curve which closely follows the envelope of the high resolution CH<sub>4</sub> spectrum already shown earlier. There is a strong peak in modulation index at 1.666 μm, corresponding to the Q-branch of the 2ν<sub>3</sub> absorption band of CH<sub>4</sub>.

The effect of changing the filter bandwidth, yet keeping its center wavelength fixed, will now be considered. It is expected that, if the filter band were initially to be centered slightly away from one of the gas absorption lines then, as the filter bandwidth is increased, the modulation index will increase rapidly to a maximum, as the line is included, and then decrease, as the average absorption reduces, this reduction being mainly due to the inclusion of spectral regions having little or no absorption. This is indeed shown to be the case and figure 4 shows that, as expected, the maximum

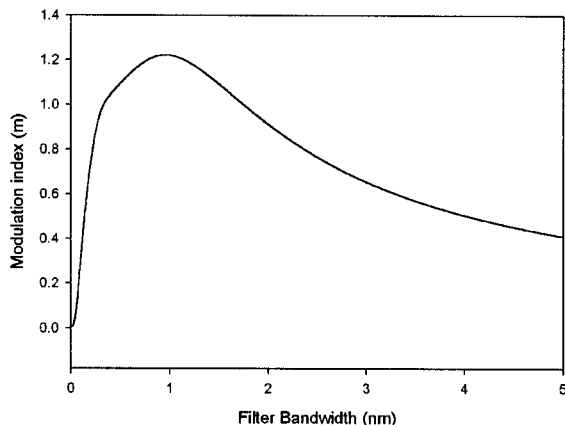


**Figure 4.** Modulation index vs. filter bandwidth assuming reference and measurement cells, containing 100% CH<sub>4</sub> at 1.013 Bar and 20 °C, of length 1m at STP, and selection filter center wavelength of 1666 nm.

modulation index is achieved at a relatively narrow bandwidth (0.96 nm). The maximum would be at a much narrower bandwidth if the filter were to have been initially centered on a line.

The full dependence of modulation index on the center wavelength and bandwidth of the optical filter is shown in a 3-D plot in figure 5. As expected, at very narrow filter bandwidths, the response closely follows the outline of the gas absorption spectrum, leading to many local maxima and minima (please note that many peaks have been omitted by under-sampling to avoid "cluttering" the graph shown in figure 5, so only 4 peaks remain to illustrate the effect. If this had not been done, most of the graph would be blackened by the high density of lines. There is essentially no effect on the graphical results where the contour is smoother). At larger bandwidths, the response 'averages' the effects of many absorption lines and a more uniform contour is seen. It is only under these conditions that the real advantages of CoSp, such as selectivity and freedom from undesirable narrow-band coherent light effects (e.g. "speckle", interference, modal noise in fibers etc.) can be realized. It will be shown later that, as expected, the signal to noise ratio also improves when more gas lines are included, as more energy from the broadband source is effectively utilized. Because of this, a wider choice of filter bandwidth will be chosen for this measurement analysis and the reasons will be justified later.

#### *4.3. Calculation of dependence of modulation index on measurement cell gas concentration*

It is often desired to detect a target gas at low concentration levels. It is therefore useful to model the modulation index at low concentrations of CH<sub>4</sub> in the measurement gas cell. For this, a much wider (100 nm) bandwidth optical filter will be chosen,

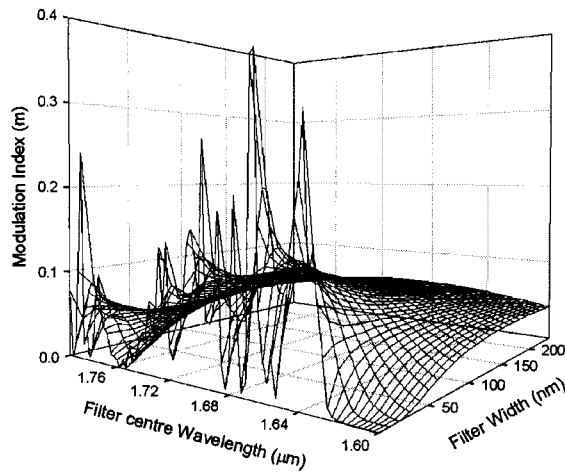


**Figure 5.** Modulation index as a function the center wavelength and bandwidth of the optical filter The broad range of strong absorption lines results in a very complex modulation index response. Note that not all peaks are shown when the narrowest filter bandwidths are analyzed, as this would cause too much "clutter" and make the plot unreadable. This is achieved by under-sampling the data for these narrow-band conditions

centered at  $1.666\mu\text{m}$  (It will be shown later that a filter with 100 nm bandwidth gives a substantially improved SNR at the measurement detector). Figure 6 shows that the modulation index response becomes non-linear at high concentrations of  $\text{CH}_4$ , due to the strong absorption of this gas. The expected nearly-linear dependence of modulation index on concentration at low levels ( $<1\%$  vol/vol) is shown in figure 7. Keabian et al. [10] have presented **experimental** results for  $\text{NO}_2$  gas detection which also showed non-linear behavior at higher concentrations for this gas, but they do not appear have published any **theoretical** work to predict this behavior.

## 5. Signal to Noise Ratio (SNR) Analysis

In order to determine the sensitivity limits of a CoSp system, the SNR variation has been calculated in terms of both the received optical power and the chosen characteristics of the optical filter.

This shows that (see below) choosing a very narrow optical filter bandwidth is not an optimal choice for a good SNR. If a broadband optical source is used, the received optical power increases, giving improved sensitivity. In addition, when a larger part of the absorption spectrum of the gas is used for the measurement, there is an improvement (i.e reduction) in the level of rejection of crosstalk from contaminant gas, and speckle interference effects are expected to reduce.

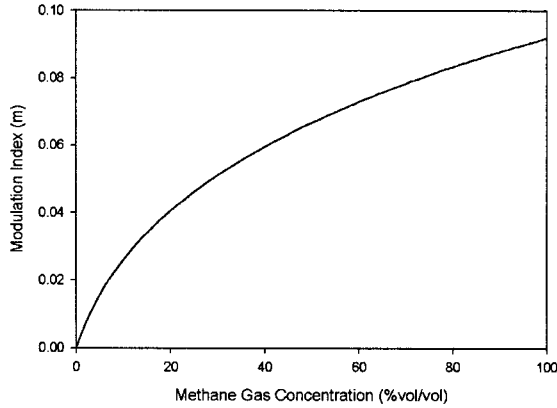


**Figure 6.** Modulation index as a function of  $\text{CH}_4$  concentration (%vol/vol) in the measurement cell. Reference and measurement cells are both of 1m length and reference cell contains 100%  $\text{CH}_4$  at 293 K and 1.013 Bar. A Gaussian-shaped optical filter, with a bandwidth of 100 nm, at a center wavelength of  $1.666\mu\text{m}$  was assumed.

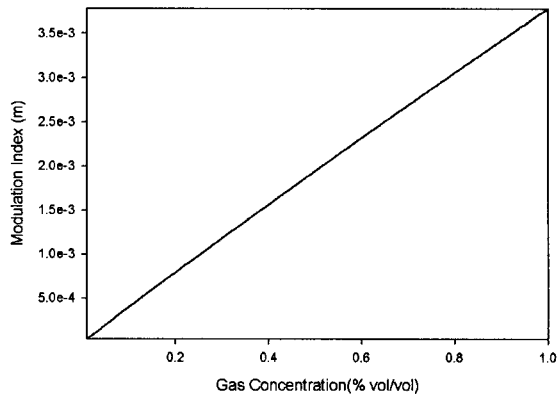


**Figure 7.** Modulation index as a function of  $\text{CH}_4$  content at low concentrations (%vol/vol) in the measurement cell. Reference and measurement cells are both of 1 m length and the reference cell contains 100%  $\text{CH}_4$  at a temperature of 293 K and a pressure of 1.013 Bar. A Gaussian-shaped optical filter, with bandwidth of 100 nm, at a center wavelength of  $1.666\mu\text{m}$ , is assumed.

### 5.1. Calculations of expected signal to noise ratio in measurement

The SNR performance of the system will now be predicted, assuming that noise arises only from fundamental photon noise at the optical detector diode and from thermal noise in the optical receiver circuit. It is assumed the optical receiver is an extended-GaInAS PIN detector, followed by a  $10\text{M}\Omega$  transimpedance amplifier (i.e. the feedback resistor,  $R_{Feedback}$  is  $10\text{M}\Omega$ ). The shot and thermal noise sources are expressed by equations 2 and 3 respectively:



$$I_{ShotNoise} = \sqrt{2qI_{Sig}B} \quad (2)$$

$$I_{ThermalNoise} = \sqrt{\frac{4kTB}{R_{Feedback}}} \quad (3)$$

where  $q$  is the electronic charge,  $k$  is the Boltzmann constant,  $T$  is the absolute temperature (assumed to be room temperature, 293 K),  $I_{Sig}$  is the DC output current of the output detector and  $B$  is the post-detection electronic processor bandwidth that limits the noise contribution by signal averaging. The post-detection integration time constant, for averaging the output signals, was assumed to be 10 s, corresponding to an equivalent value of 0.016 Hz for the noise bandwidth,  $B$ .

As already mentioned above, maximizing the modulation index is not the only important criterion for optimizing such a system, as the signal to noise ratio at the measurement detector is also a key practical parameter. The SNR is defined as the ratio of the detected optical modulation signal to the total received noise level, the latter being calculated by incoherently combining the expressions for shot and thermal noise sources.

In figure 8, the SNRs expected are shown, as a function of optical filter bandwidth. As stated above the post-detection integration time constant, for averaging the output signals, was assumed to be 10 s, corresponding to an equivalent value of 0.016 Hz for the noise bandwidth,  $B$ . The separate curves show results corresponding to several different choices for the detected optical power spectral densities, ranging from 10 nW nm<sup>-1</sup> to 70 nW nm<sup>-1</sup>. (NOTE: The values of optical power spectral densities shown in these plots are those that would occur if there were to be no gas absorption in the measurement cell)

At first, the SNR ratio can be seen to improve with increasing filter bandwidth, because of the absorption effects of more gas absorption lines being included. However, eventually, as the filter bandwidth starts to extend beyond the region of strong absorption bands, the additional light, that does not suffer significant absorption, will merely increase the photon noise and hence, cause the SNR to decrease. If the SNR figures of the type shown in figure 8 can easily be converted to derive the Noise-Limited Detection Sensitivity (NLDS) for methane detection. This is achieved by taking the peak SNR values, assuming much lower concentrations in the measurement cell, and extrapolating the result to find the CH<sub>4</sub> concentration at which the expected SNR would be 1. Performing this analysis, the predicted NLDS figures were found to be 0.8 ppm, 0.4 ppm and 0.3 ppm, when assuming received power spectral densities of 10, 40 and 70 nW nm<sup>-1</sup> respectively.

The optimum SNR is achieved using a filter width of approximately 150 nm, although around the maximum it can be seen that there is only a very gradual variation of the SNR with filter bandwidth over a wide range. Note that, achieving an optimum SNR requires a much wider choice of filter bandwidth than that required to maximize the modulation index.

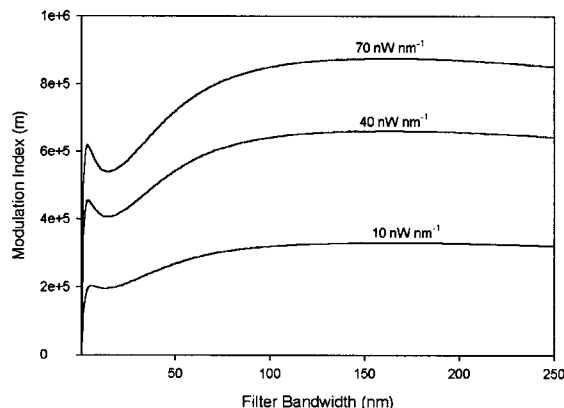


**Figure 8.** Predicted variation in SNR at different detected spectral power densities, ranging from  $10 \text{ nW nm}^{-1}$  to  $70 \text{ nW nm}^{-1}$ , as a function of the bandwidth of a Gaussian-shaped optical filter (assumed to be centered at  $1.666 \mu\text{m}$ ). The post-detection integration time constant for these measurements was assumed to be 10 s, corresponding to an equivalent noise bandwidth of 0.016 Hz. Reference and measurement gas cells are of 1 m length and contain only  $\text{CH}_4$  gas, at 1.013 Bar and  $20 \text{ }^\circ\text{C}$ .

The 3-D graph in figure 9, calculated using similar conditions to those used to produce figure 8, shows the effect of changing the center wavelength and bandwidth of the optical filter, assuming that a power spectral density of  $10 \text{ nW nm}^{-1}$  is received at the detector. This graph also shows, as was the case with the 2-D plots in figure 8, that, to optimize the SNR, the optimal filter bandwidth should be around 150 nm. It also verifies that the tolerances for the optical filter parameters are not very critical for achieving a good SNR, once a filter above 70 nm bandwidth is chosen. A choice of 100 nm bandwidth for the optical filter, as will be shown later, gives good SNR and also includes many gas lines to enhance "fingerprinting" and reduce "speckle" coherence effects. It will now be shown that this also represents a practical choice when cross contamination effects of water vapor are included.

### *5.2. Cross-sensitivity to water vapor*

As a final consideration, the cross-sensitivity of the sensor to a selected contaminant gas will be examined. For this analysis, water vapor was chosen as the most likely, and perhaps most difficult contaminant to deal with in practical systems. It is not only very difficult to exclude in practice, being adsorbed readily in polymer materials, but it also has very many spectral absorption bands occurring over a large part of the visible and near-infrared regions. The CoSp method has the useful property of having high selectivity, even when exposed to a pollutant gas whose absorption bands overlap with the target gas, provided that the absorption lines of the two gases do not exactly coincide. This selectivity advantage arises because of the correlation function behavior

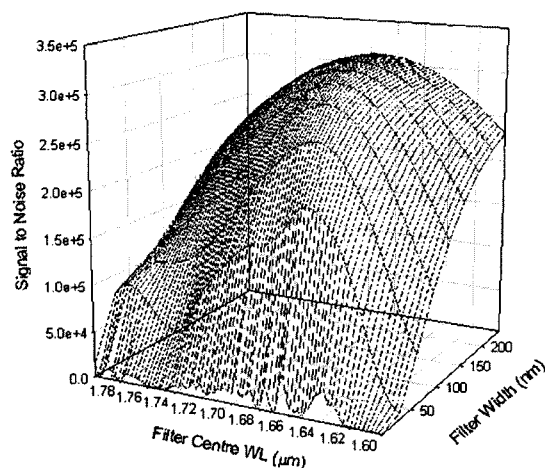


**Figure 9.** SNR in measurements as a function of selection filter choice. It was assumed that  $10 \text{ nW nm}^{-1}$  spectral power would be received at the detector if the measurement gas cell had no absorption (other parameters were as in figure 8).

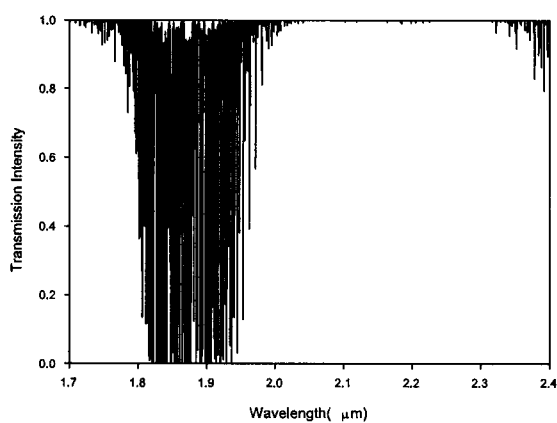


**Figure 10.** Transmission spectrum of water vapor over a 1 m path length at a temperature of 293 K and a pressure of 1.013 Bar (transmission data obtained from HITRAN database).

described by equation 1. The expected response of the  $\text{CH}_4$  sensor to water vapor, a likely contaminant species with some absorption overlap with the spectrum of  $\text{CH}_4$ , will therefore now be quantified. Firstly, the transmission spectrum of water vapor will be shown (figure 10).

The predicted cross-sensitivity behavior of the  $\text{CH}_4$  sensor to water vapor is shown in figure 11, where the modulation index, expected when the measurement cell contains water vapor, is plotted as a function of optical filter bandwidth. Optical filters having the optimum center wavelength of  $1.666 \mu\text{m}$ , for  $\text{CH}_4$  detection, were chosen. This

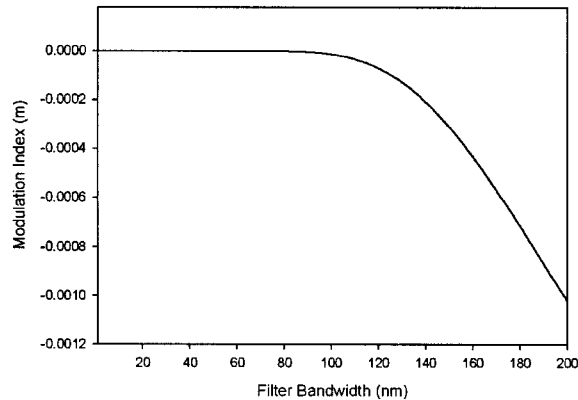


**Figure 11.** Modulation index response to contaminant H<sub>2</sub>O. This assumes a CoSp system using a Gaussian shaped filter centered at 1.666  $\mu\text{m}$ , 1 m long reference containing 100% CH<sub>4</sub> at 293 K and 1.013 Bar. For crosstalk it was assumed that the measurement cell contained 5% H<sub>2</sub>O vapor (0.05 Bar partial pressure) at a temperature of 293 K and a pressure 1.013 Bar.

shows the sensor starts to become significantly sensitive to water vapor only when an optical filter bandwidth much in excess of 100 nm is used. The cross-sensitivity is generally small, that from 5% water vapor having a negative value (signal change is in the opposite direction to the methane absorption, due to interleaving absorption lines) and has a magnitude equivalent to only 21 ppm CH<sub>4</sub> when a 100 nm wide optical filter is used. This rises to 9600 ppm CH<sub>4</sub> when a optical filter having an excessively large bandwidth, vis 200 nm, is used. However, if were to be assumed that CoSp were not used, and a simple absorption-loss system is analyzed, the expected crosstalk is far worse. Simple integration of the corresponding absorption curves, over the same 100 nm filter spectrum, shows that 5% water vapor would give crosstalk signals corresponding to 200 ppm CH<sub>4</sub>, a crosstalk factor nearly 10 times worse than for the CoSp method!

### 5.3. Conclusions

We have produced a generic theoretical model for gas detection systems using the CoSM scheme for absorption based CoSp. The model has been used to predict the responsivity, noise-limited sensitivity and crosstalk performance of a CH<sub>4</sub> sensor. The optimal component characteristics for best signal-to-noise and selectivity to CH<sub>4</sub> have been predicted. This work has shown that, as expected, the modulation-index response of an absorption based CoSp system is strongly dependant on the characteristics of the optical filter chosen. For optimum modulation index (measurement contrast), an optical filter having a center wavelength of 1.666  $\mu\text{m}$  and a bandwidth below 1 nm would be chosen, but this would select too few lines to give the selectivity and other advantages of CoSp. We have shown that, when other key aspects, such as achieving a good SNR and reducing the "speckle" interference effects that can cause modal noise in fibres, are taken

into account, it is generally better to use an optical filter of somewhat higher bandwidth. Fortunately, following an initial peak, the modulation index, or measurement contrast, does not drop very rapidly when wider filter bandwidths are chosen.

The best SNR is predicted using a filter of 150 nm bandwidth, whence a noise limited detection sensitivity (NLDS) of 0.8 ppm CH<sub>4</sub> is expected. This is assuming use of 1 m cells, with 100% gas in the reference cell and a received spectral power density at the detector of 10 nW nm<sup>-1</sup>. The (NLDS) would improve to 0.3 ppm, if a greater received spectral power density of 70 nW nm<sup>-1</sup> were achieved.

The sensor is shown to be highly selective in the presence of water vapor. When a 100 nm bandwidth optical filter is chosen, the crosstalk response to 5% water vapor has a negative value (signal change is in the opposite direction to the methane absorption, due to interleaving absorption lines) and is equivalent to only 21 ppm CH<sub>4</sub>. By way of comparison, conventional absorption systems (including photo-acoustic types) might expect a crosstalk response of the order of 200 ppm, a factor of 10 times worse.

- [1] R. Goody. Cross-correlating spectrometer. *Journal of the Optical Society of America*, 58(7):900–908, 1968.
- [2] W. F. Herget, J. A. Jahnke, D. E. Burch, and D. A. Gryvnak. Infrared gas-filter correlation instrument for in situ measurement of gaseous pollutant concentrations. *Applied Optics*, 5:1222–1228, 1976.
- [3] T. Kobayashi, M. Hirana, and H. Inaba. Remote monitoring of no<sub>2</sub> molecules by differential absorption using optical fibre link. *Appl. Opt.*, 20(5):3279, 1981.
- [4] A. Hordvik, A. Berg, and D. Thingbø. A fibre optic gas detection system. In *Proc. 9th Int. Conf. on Opt. Comms., 'ECOC 83'*, page 317, 1983.
- [5] K. Chan, H. Ito, and H. Inaba. An optical fibre-based gas sensor for remote absorption measurements of low-level methane gas in the near-infrared region. *J. Lightwave Tech.*, LT-2,:234, 1984.
- [6] S. Stueflotten, T. Christensen, S. Iversen, J. O. Hellvik, K. Almas, and T. Wien. An infrared fibre optic gas detection system. In *Proc. OFS-94 int conf*, page 87, 1986.
- [7] J. P. Dakin and H. O. Edwards. Progress in fibre-remoted gas correlation spectroscopy. *Special issue of Optical Engineering*, 31:1616–1620, 1992.
- [8] H. O. Edwards and J. P. Dakin. Gas sensors using correlation spectroscopy compatible with fibre-optic operation. *Sens. & actuators B,: Chem*, 11:9, 1993.
- [9] J. P. Dakin, H. O. Edwards, and B. H. Weigl. Progress with optical gas sensors using correlation spectroscopy. *Sens. & actuators B,: Chem*, 29:87, 1995.
- [10] P. L. Kebabian, K. D. Annen, T. A. Berkoff, and A. Freedman. Nitrogen dioxide sensing using a novel gas correlation detector. *Measurement Science and Technology*, 11:499–503, 2000.
- [11] J. P. Dakin, M. J. Gunning, P. Chambers, and Z. J.Xin. Detection of gases by correlation spectroscopy. *Sens. & actuators B,: Chem*, 90:124–131, 2003.
- [12] P. Chambers, E. A. Austin, and J. P. Dakin. Model to predict the response of correlation spectroscopy gas detection systems for ch<sub>4</sub>. In *Proc. OFS-16, IEICE*, pages 738–741, 2003.